

# Principal Boundary on Riemannian Manifolds

June 29, 2022

Zhigang Yao  
 Department of Statistics and Applied Probability  
 21 Lower Kent Ridge Road  
 National University of Singapore, Singapore 117546  
 email: zhigang.yao@nus.edu.sg

Zhenyue Zhang  
 Department of Mathematics  
 Zhejiang University, Yuquan Campus  
 Hangzhou 310027 China  
 email: zyzhang@math.zju.edu.cn

## Abstract

We revisit the classification problem and focus on nonlinear methods for classification on manifolds. For multivariate datasets lying on an embedded nonlinear Riemannian manifold within the higher-dimensional space, our aim is to acquire a classification boundary between the classes with labels. Motivated by the principal flow [14], a curve that moves along a path of the maximum variation of the data, we introduce the principal boundary. From the classification perspective, the principal boundary is defined as an optimal curve that moves in between the principal flows traced out from two classes of the data, and at any point on the boundary, it maximizes the margin between the two classes. We estimate the boundary in quality with its direction supervised by the two principal flows. We show that the principal boundary yields the usual decision boundary found by the support vector machine, in the sense that locally, the two boundaries coincide. By means of examples, we illustrate how to find, use and interpret the principal boundary.

## 1 Introduction

Most of the classification methodology in high dimensional data analysis is deeply rooted in methods relying on linearity. Modern data sets often consist of a large number of observations, each of which is made up of many features.

Manifold data arises in the sense that the sample space of data is fundamentally nonlinear. Instead of viewing the features of any observation as a point in a high-dimensional space, it is more convenient to assume the data points lie on an embedded lower-dimensional non-linear manifold within the higher-dimensional space. The lower-dimensional manifold structure can usually be interpreted from at least two scenarios: 1) the physical data space is an actual manifold; 2) the underlying data structure can be approximated by a close manifold. In the former scenario, the data space is usually known, and it can be further seen as data in shape space [10], e.g., earthquake coordinates, leaf growth pattern, and data with nonlinear constraints thus forced to lie on a manifold. In the latter scenario, the manifold is uncovered from the data set by a non-linear dimensionality reduction technique referred to as the manifold learning method [17, 1, 20], and, thus, it is considered unknown.

In this work, we consider the classification problem and design the nonlinear methods which perform as a boundary for classifying data sets lying on manifolds. Throughout, we mainly focus on the known “manifold” case; that is, the embedding is known. This problem has become increasingly relevant, as many real applications such as medical imaging [5, 18] and computer vision produce data [15, 16] in such forms. This encourages researchers to do the analysis directly on the manifold rather than in the Euclidean space or the enlarged Euclidean space using basis expansions. The rationale behind this is that the metric on the manifold is much more reasonable than that in the Euclidean space, if the data resides on manifolds. However, the methodology defined upon manifold space for classification is still lacking. To perform reliable classification for data points on manifolds, a strategy of developing statistical tools, such as the nonlinear classification boundary, in parallel with their Euclidean-counterparts, is significantly relevant.

Though we have seen tremendous effort in developing statistical procedures for classification problems, the major part has been focused on constructing the separating hyperplane between two classes in the Euclidean space. The optimality is essentially restricted to finding *linear* (affine) hyperplanes that separate the data points as best as possible. Among them, linear discriminant analysis (LDA), or the slightly different logistic regression method, manifest themselves in the case of seeking the hyperplane by minimising the so-called discriminant function, and thus they are able to trace out a linear boundary separating the different classes. Further to linear boundary, the support vector machine (SVM) finds a seemingly different separating hyperplane; that is, the hyperplane is actually found (up to some loss function), not in its original feature space, but in an enlarged space, by transforming the feature space into an unknown space via basis functions. In this sense, SVM is only capable of producing the namely nonlinear boundary with respect to the original space. This being said, a direct extension of SVM while retaining its use as a classifier when it comes to the manifold is not straightforward.

There have been a number of pieces of research on the statistical methods on manifolds over the past decades, centring around finding the main modes of variation [4, 6] in the data, or finding a manifold version of the principal

components for the data [9, 3, 7, 12, 2, 11, 8], in terms of dimension reduction. However, none of them seem to be adaptable in deriving a boundary on a manifold, due to their “non curve-fitting” nature. Recently, the principal flow [14] has been proposed as a one-dimensional curve, defining on the manifold, such that it attempts to follow the main direction of the data locally, while still being able to accommodate the “curve fitting” characteristic on the manifold. The variational principal flow [13] incorporates the level set method to obtain a fully implicit formulation of the problem. The principal sub-manifold [19] extends the principal flow to a higher dimensional sub-manifold. It is natural to raise the question as follows: whether anything interesting can be found that can separate the data directly on the manifold, without attempting to formulate the same problem in another unknown space?

We explore the limitations inherent in the problem when trying to find such a boundary. Inspired by the principal flow, we consider generalisations of the classification boundary on Riemannian manifolds. We do not intend to merely search a nonlinear boundary, directly on the manifold, that satisfies a certain optimisation condition with respect to the data points. Rather, our idea is to trace a boundary out of the two principal flows from the two classes, and at the same time retain some canonical interpretation for the boundary. Our intuition is that, as the two principal flows represent the mean trend of the two classes, in order to classify the points, it is enough to separate the two flows in some optimal way. This means that one does not need to consider the data points beyond the two flows on each side anymore, as they are irrelevant to the classification, provided that we can separate the flows well. Naturally, because of the two principal flows, the process of constructing the boundary can be supervised, in the sense that the boundary grows itself by borrowing strength from the two principal flows. To achieve this, the key insight is the margin, a measure of distance between the target boundary and the two principal flows, subject to the presence of noise originating from each class. In principal, an optimal boundary can be framed by maximising the margin between the target boundary and the two corresponding principal flows. The optimisation involved therein can be relaxed by fine-tuning the subspace of the vector field from the two principal flows, up to their parallel transport on the manifold. From this perspective, the boundary retains the characteristic of being principal, in the sense that at each point of the boundary, it points to the direction calculated over the two directions of the vector field from the two principal flows. This finally results in a classification boundary which is named as the principal boundary, drawing a relation to the principal flow.

We demonstrate how the problem of obtaining the principal boundary can be transformed to a well-defined integration problem in Section 3.2, with a motivation and an introduction of the margin in Section 3.1, which plays a key role in defining the boundary. The formal definition of a principal boundary is given in Section 3.2. We show that on the manifold, the principal boundary reduces to the SVM boundary, at least locally; that is, the segment of the principal boundary coincides with that of SVM. Section 5 contains the property

of the boundary with a detailed analysis of the relation between the boundary and SVM. Generally speaking, our formulation of the boundary is feasible for any Riemannian manifold, provided that the geodesic is unique, although an unknown geodesic might increase the complexity in computation.

The remaining part of the paper is organised as follows. We start with a brief introduction of the principal flow (Section 2.2-2.3) with a modified vector field and a modified principal flow. Section 3 is the Methodology section. Section 4 investigates an implementable algorithm for determining the principal boundary. Section 5 gives all the technical details of the equivalence of the boundary and SVM. In Section 6, we illustrate the principal boundary by means of simulated examples. We end the paper with a discussion.

## 2 The Problem

We are interested in the following problem: let  $\mathcal{M}$  be a Riemannian manifold in  $\mathbb{R}^d$  with the dimension  $m < d$ . Let  $x_{1,i}$  ( $i = 1, \dots, n_1$ ) be the data points on  $\mathcal{M}$  with label  $y_{1,i} = +1$  ( $i = 1, \dots, n_1$ ) and  $x_{2,i}$  ( $i = 1, \dots, n_2$ ) be the data points on  $\mathcal{M}$  with label  $y_{2,i} = -1$  ( $i = 1, \dots, n_2$ ). We are looking for a classification boundary, say  $\gamma$ , on  $\mathcal{M}$ , that is as wide as possible between the data points for class 1 and -1.

The heuristic behind the principal boundary is that first we construct the two mean flows  $\gamma_1$  and  $\gamma_2$  of the data points  $x_{1,i}$  and  $x_{2,i}$ , respectively. Each mean flow represents the principal direction of the data variation for each class on  $\mathcal{M}$ . Second, the classification problem can now be rephrased as finding a flow  $\gamma$ , lying between  $\gamma_1$  and  $\gamma_2$ , which separates the two as well as possible.

The two mean flows are in fact called principal flows. Before we continue, let us digress slightly and review the principal flow.

### 2.1 Preliminaries

Let  $x_i$  ( $i = 1, \dots, n$ ) be  $n$  data points on a complete Riemannian manifold  $\mathcal{M}$  of dimension  $m$ , where  $m < d$ , embedded in the linear space  $\mathbb{R}^d$ .

We assume that a differentiable function  $F : \mathbb{R}^d \rightarrow \mathbb{R}^m$  always exists, such that

$$\mathcal{M} := \{x \in \mathbb{R}^d : F(x) = 0\}.$$

For each  $x \in \mathcal{M}$  the tangent space at  $x$  will be denoted by  $T_x\mathcal{M}$ , then  $T_x\mathcal{M}$  is characterised by the equation

$$T_x\mathcal{M} = \{y : DFy = 0, y \in \mathbb{R}^d\}.$$

Thus,  $T_x\mathcal{M}$  is in fact a *vector space*, the set of all tangent vectors to  $\mathcal{M}$  at  $x$ , which essentially provides a local vector space approximation of the manifold  $\mathcal{M}$ .

By equipping the manifold with the tangent space, we define two mappings back and forth between  $T_x\mathcal{M}$  and  $\mathcal{M}$ : 1) the exponential map, well defined in terms of geodesics, is the map:

$$\mathbf{exp}_x : T_x\mathcal{M} \rightarrow \mathcal{M} \quad (1)$$

by  $\mathbf{exp}_x(v) = \gamma(\|v\|)$  with  $\gamma$  a geodesic starting from  $\gamma(0) = x$  with initial velocity  $\dot{\gamma}(0) = v/\|v\|$  and  $\|v\| \leq \delta$ , and 2) the logarithm map (the inverse of the exponential map), is locally defined at least in the neighborhood of  $x$ ,

$$\mathbf{log}_x : \mathcal{M} \rightarrow T_x\mathcal{M}. \quad (2)$$

Here, the  $\mathbf{exp}$  and  $\mathbf{log}$  are defined on a local neighborhood of 0 and  $x$  such that they are all well-defined, away from the cut locus of  $x$  on  $\mathcal{M}$ .

Let  $x, y \in \mathcal{M}$ . Denote all (piecewise) smooth curves  $\gamma(t) : [0, 1] \rightarrow \mathcal{M}$  with endpoints such that  $\gamma(0) = x$  and  $\gamma(1) = y$ . The *geodesic distance* from  $x$  to  $y$  is defined as

$$d_{\mathcal{M}}(x, y) = \inf \ell(\gamma) \quad (3)$$

where  $\ell(\gamma) = \int_{[0,1]} \|\dot{\gamma}(t)\| dt$ . Minimising (3) yields the shortest distance between the two points  $x$  and  $y$  in  $\mathcal{M}$ .

## 2.2 Definition of principal flow

**Definition 2.1** *The principal flow  $\gamma$  of  $x_i$  ( $i = 1, \dots, n$ ) is defined as the union of the two curves,  $\gamma^+$  and  $\gamma^-$ , satisfying the following two variational problems, respectively*

$$\gamma^+ = \arg \sup_{\gamma \in \Gamma(x_0, v_0)} \int_{\gamma} \langle \dot{\gamma}, W(\gamma) \rangle ds \quad (4)$$

$$\gamma^- = \arg \inf_{\gamma \in \Gamma(x_0, -v_0)} \int_{\gamma} \langle \dot{\gamma}, W(\gamma) \rangle ds \quad (5)$$

where  $x_0$  is the starting point and  $v_0$  is the a unit vector at  $x_0$ . The point  $x_0$  can be chosen as the Fréchet mean  $\bar{x}$  of  $x_i$  ( $i = 1, \dots, n$ ) such that

$$\bar{x} = \operatorname{argmin}_{x \in \mathcal{M}} \frac{1}{n} \sum_{i=1}^n d_{\mathcal{M}}^2(x, x_i),$$

or any other point of interest. Note that  $\Gamma(x_0, v_0)$  is the set of all non-intersecting differentiable curves on  $\mathcal{M}$ .

Technically, the principal flow incorporates two ingredients: a local covariance matrix and a vector field.

For the data point  $x_j$ , choose a neighborhood  $\mathcal{N}(x_j, h)$  of  $x_j$  with a radius  $h$ , defined as

$$\mathcal{N}(x_j, h) = \{x_i : d_{\mathcal{M}}(x_i, x_j) \leq h\}.$$

Accordingly, the local covariance matrix is defined as

$$\Sigma_h(x_j) = \frac{1}{\sum_i \kappa_h(x_i, x_j)} \sum_i \mathbf{log}_{x_j}(x_i) \otimes \mathbf{log}_{x_j}(x_i) \kappa_h(x_i, x_j)$$

where  $y \otimes y := yy^T$ ,  $\kappa_h(x_i, x_j) = K(h^{-1}d_{\mathcal{M}}(x_i, x_j))$  with a smooth non-increasing uni-variate kernel  $K$  on  $[0, \infty)$ .

Let  $B \subset \mathcal{M}$  be a connected open set covering  $x_i$  ( $i = 1, \dots, n$ ) and such that  $\mathbf{log}_x y$  is well defined for all  $x, y \in B$ . Assume that  $\Sigma_h(x_j)$  has distinct first and second eigenvalues for all  $x \in B$ . The vector field is defined in the way that the first eigenvector  $e_1(x_j)$  (or eigenvalue  $\lambda(x_j)$ ) of  $\Sigma_h(x_j)$  is extended to a vector field  $W := \{W(x) \equiv v(x_j) : x \in \mathcal{N}(x_j, h)\}$  where  $v(x_j) = e_1(x_j)$ ; that is, for any  $x \in \mathcal{N}(x_j, h)$ , we have

$$\Sigma_h(x)W(x) = \lambda(x)W(x) \text{ (i.e., } W(x) \in W \text{)}. \quad (6)$$

In the meanwhile, it has been proved that  $W : \mathcal{N}(x_j, h) \rightarrow \mathbb{R}^d$  is a differentiable mapping with  $W(x)$  being independent of the local coordinates of the tangent space  $T_x \mathcal{M}$ .

It can be seen that the curve  $\gamma^+$  starts at  $x_0$  and follows the direction of the vector field and the curve  $\gamma^-$  starts at  $x_0$  and goes in the opposite direction of the vector field. Thus, the integral for  $\gamma^-$  is negative, which explains why the infimum appears in its definition.

Under the principal flow definition, we can define  $\gamma_1$  of  $x_{1,i}$  ( $i = 1, \dots, n_1$ ) as the union of  $\gamma_1^+$  and  $\gamma_1^-$ , and  $\gamma_2$  of  $x_{2,i}$  ( $i = 1, \dots, n_2$ ) as the union of  $\gamma_2^+$  and  $\gamma_2^-$ . For convenience, we will only consider the flow  $\gamma_1^+$  in (1) of Definition (2.1), and re-name it as  $\gamma_1$ . By symmetry, the solution to the flow  $\gamma_1^-$  in (2) of Definition (2.1) can be carried out in the same way. Similarly, we will restrict the discussion to  $\gamma_2^+$  and re-name it as  $\gamma_2$ .

### 2.3 Modified principal flow

The principal flow relies heavily on the vector field. However, the original definition (see (6)) of the vector field strictly constructs the direction of every point in the field as solely pointing to the eigenvector of the local covariance matrix. This definition could be problematic when we need a much delicate field for the flow. To be exact, for each point belonging to a neighbourhood where the field is calculated, it can also be in other neighbours. It turns out that we will need to modify the vector field for the principal boundary, since the vector field plays quite a crucial role in the problem.

We will equip a vector field for each training sample (say  $x_j$ ) in the data  $\{x_i\} (i = 1, \dots, n)$ . For samples in each neighbourhood, say  $\mathcal{N}(x_i, h)$ , determine a locally dominate or principal vector  $v_i$  by the local tangent PCA.

A sample  $x_j$  can be the neighbour of multiple points. Let  $I_j$  be the index set of neighbour sets  $\mathcal{N}(x_i, h)$  that holds  $x_j$  as a neighbour. The modification of vector field amounts to overall effect of holding multiple neighbourships for a point. To achieve this, it is very natural to equip a vector for  $x_j$  as a weighted

sum of the locally principle vectors  $\{v_i : i \in I_j\}$ . Let  $c_i$  be the mean of  $\mathcal{N}(x_i, h)$  when we determine  $v_i$ . Then, we assign the vector  $v(x_j)$  for  $x_j$ , which is the projection  $v_{\mathcal{M}}(x_j)$  of the weighted sum

$$v(x_j) = \sum_{i \in I_j} w_{ij} v_i, \quad w_{ij} = \frac{\exp(-d_{\mathcal{M}}(x_j, c_i))}{\sum_{i \in I_j} \exp(-d_{\mathcal{M}}(x_j, c_i))}$$

onto the manifold at  $x_j$ .

As soon as we have a vector field constructed above, a principal flow  $\gamma$  of the given data set  $\{x_i\}$  is defined by

$$\gamma = \arg \sup_{\gamma \in \Gamma(x_0, v_0)} \int_{\gamma} \left\langle \dot{\gamma}, \sum_{x_j \in \mathcal{N}(p, h)} v(x_j) \right\rangle ds \quad (7)$$

That is, at the point  $p \in \gamma$ , the tangent  $\dot{\gamma}$  should match the vector field of samples in the neighbourhood  $\mathcal{N}(p, h)$ . To differentiate from the principal flow in Definition 2.1, we call  $\gamma$  the modified principal flow.

### 3 Methodology

Now we get back to the original question; that is, given two principal flows  $\gamma_1$  and  $\gamma_2$  determined from two data sets  $x_{1,i}$  and  $x_{2,j}$ , can we find a curve, say  $\gamma$ , that can be used as a classification boundary between the two classes?

Strictly speaking, many  $\gamma$ s in  $\Gamma(x_0, v_0)$  could exist, that separate two classes of data. Therefore, by using the term the classification boundary, we refer to the best one. We present the general idea of constructing such a boundary here, leaving the formal introduction in Section 3.2: let the  $\gamma$  start from  $\gamma(0)$  and move infinitesimally in the direction of  $\dot{\gamma}(0)$ . At this moment, we assume that both  $\gamma(0)$  and  $\dot{\gamma}(0)$  are carefully chosen so that the flow moves in the correct direction. Once the first move has been made, it may no longer make sense to continue moving in the same direction  $\dot{\gamma}(0)$ . One may ask, then, in what direction should we move? Obviously, we should not move either towards  $\gamma_1$  or  $\gamma_2$ , since this would cause  $\gamma$  to move close to either of the two flows. To update the direction, a natural strategy that plays an important role in building the boundary is to let  $\gamma$  move in a direction supervised by  $\gamma_1$  and  $\gamma_2$ ; that is, we follow the vector field inherited from  $\gamma_1$  and  $\gamma_2$ , then move by choosing the proportional amount of vector field from  $\gamma_1$  and  $\gamma_2$  each time. Indeed, the right amount of vector field to choose for the next move is essentially an optimisation problem, the derivation of which will be discussed in the next section. This being said, the intuitive version of such a boundary is not unique in the sense that a parallel curve satisfying the same condition always exists, and this can be seen by varying the initial point. To achieve the classification, let us view the problem slightly differently: note that it is only the points lying in between  $\gamma_1$  and  $\gamma_2$  that could influence  $\gamma$ , so a very straightforward approach is to choose the tangent vector for the next move along the direction that creates the biggest

margin between the data points for class +1 and -1. Under this rationale, iterating the process would approximately trace out an integral curve that is not only proportionally compatible to the vector fields of the two flows at each point, but more importantly, the curve will separate the margin, which therefore can be considered as a classification boundary.

### 3.1 Margin

At each point  $p \in \gamma$ , the tangent vector of  $\gamma$  at  $p$  should be the locally principal vector of samples in  $\mathcal{N}(p, h)$ . Suppose that distinct first and second largest eigenvalues of the local covariance matrix of the centered samples for  $\mathcal{N}(p, h)$  exist. The principal vector is the dominant eigenvector in  $\mathcal{N}(p, h)$ , corresponding to its largest eigenvalue  $\lambda_1$ . The local PCA also determines the second largest eigenvalue value  $\lambda_2$ . The ratio

$$\sigma_\gamma(p) = \frac{\lambda_2}{\lambda_1} h$$

approximately indicates the largest distance of samples in the neighbourhood  $\mathcal{N}(p, h)$  deviated from the mean along the eigenvector corresponding to  $\lambda_2$ .

The distance of a point  $q$  of the manifold to the principal flow  $\gamma$  is defined as

$$d_{\mathcal{M}}(q, \gamma) = \inf_{p \in \gamma} d_{\mathcal{M}}(q, p),$$

where  $d_{\mathcal{M}}(p, q)$  is the geodesic distance between  $p$  and  $q$  on  $\mathcal{M}$ . We assume that the distance  $d_{\mathcal{M}}(q, \gamma)$  is achievable, i.e., there is a point  $p \in \gamma$  such that  $d_{\mathcal{M}}(q, p) = d_{\mathcal{M}}(q, \gamma)$ . Furthermore, we assume that the minimiser is unique. We call  $p$  as the projection of  $q$  onto  $\gamma$ , and denote it as  $p = p_\gamma(q)$  as a function of  $q$ .

Hence, if  $d_{\mathcal{M}}(q, \gamma) > \sigma_\gamma(p)$  with  $p = p_\gamma(q)$ , the gap

$$m_\gamma(q) = d_{\mathcal{M}}(q, \gamma) - \sigma_\gamma(p)$$

is a ‘soft’ margin of  $q$  for classifying  $\gamma$  in the sense that the neighbour set  $\mathcal{N}(p, h)$  locates in a side of  $q$ , at least locally. More generally, given curve  $\gamma'$  on the same manifold, if we always have positive value of  $m_\gamma(q)$  for each  $q \in \gamma'$ , then  $\gamma'$  is located on one side.

### 3.2 Principal boundary

Suppose that  $\gamma_1$  and  $\gamma_2$  are determined from the two data sets  $\{x_{1,i}\}$  and  $\{x_{2,j}\}$  respectively. We say  $\gamma_1$  and  $\gamma_2$  are separated if there is a curve  $\gamma$  such that  $\gamma_1$  and  $\gamma_2$  are on different sides of  $\gamma$ , conditioning on the margins to the two curves; that is,  $m_{\gamma_1}(q) > 0$  and  $m_{\gamma_2}(q) > 0$  for all  $q \in \gamma$ . Clearly, such a curve  $\gamma$  can correctly classify the two data sets.

If point  $q \in \mathcal{M}$  locates between  $\gamma_1$  and  $\gamma_2$ , we call the minimum of  $m_{\gamma_1}(q)$ , and  $m_{\gamma_2}(q)$  is the margin of  $q$  with respect to  $\gamma_1$  and  $\gamma_2$ , i.e.,

$$m_{\gamma_1, \gamma_2}(q) = \min \{m_{\gamma_1}(q), m_{\gamma_2}(q)\}.$$



Let  $\Gamma$  be the set of classification curve with unit speed. A good classification curve should have the margin  $m_{\gamma_1, \gamma_2}(q)$  to the two principal flows, as large as possible at each  $p \in \gamma$ . We call the ideal classification curve that has the largest value of  $m_{\gamma_1, \gamma_2}(q)$  as a *principal boundary* of the two data sets.

**Definition 3.1** A unit-speed curve  $\gamma_c \in \Gamma$  is called the *principal boundary* if it maximises the integral of the margin  $m_{\gamma_1, \gamma_2}(q)$  over  $\gamma$ . That is,

$$\gamma_c = \arg \max_{\gamma \in \Gamma} \int_{\gamma} \min \{m_{\gamma_1}(\gamma), m_{\gamma_2}(\gamma)\} ds.$$

Definition 3.1 seems to give the idea of optimising the ideal principal boundary that separates two principal flows by maximising the margin over a class of flows  $\Gamma$ . Theoretically, the class set  $\Gamma$  contains all the curves  $\gamma$  that lie in between  $\gamma_1$  and  $\gamma_2$ . This is a much broader class than is necessary to sort out a boundary from a classification point of view. Our greater interest lies in achieving such a  $\gamma_c$  over a smaller set, which is more likely accessible. Ordinarily, to find such a set one may consider the alignment between the target principal boundary and the principal flows. Hence, we will restrict our attention to a class set  $\Gamma'$ , where the correspondence among  $\gamma$  and  $\gamma_1$  or  $\gamma_2$  can be explained by a corresponding geodesic.

Assume the the projections  $p_1 = p_{\gamma_1}(q)$  and  $p_2 = p_{\gamma_2}(q)$  are one-to-one for  $q \in \gamma_c$ ; that is, a different  $q$  yields a different projection onto  $\gamma_1$  or  $\gamma_2$ . Hence, the geodesic curve  $\mathcal{C}(p_1, p_2)$  between its two projections  $p_1$  and  $p_2$  must go across the principal boundary  $\gamma_c$  at the original  $q$ . The maximisation in Definition 3.1 means that  $q \in \gamma_c$  should also be the middle point of the geodesic curve, i.e.,

$$q = \arg \max_{q' \in \mathcal{C}(p_1, p_2)} m_{\gamma_1, \gamma_2}(q'),$$

if both  $p_1$  and  $p_2$  have been pre-determined. Hence, we can equivalently define the principal boundary in a more direct way, as follows.

**Definition 3.2** A curve  $\gamma_c$  on  $\mathcal{M}$  is called the *principal boundary* of two principal flows  $\gamma_1$  and  $\gamma_2$ , if any  $q \in \gamma_c$  satisfies

- (1) the geodesic curve  $\mathcal{C}(p_1, p_2)$  between its two projections  $p_1 = p_{\gamma_1}(q)$  and  $p_2 = p_{\gamma_2}(q)$  onto  $\gamma_1$  and  $\gamma_2$  also contains the point  $q$ , and
- (2)  $m_{\gamma_1, \gamma_2}(q) = \max_{q' \in \mathcal{C}(p_1, p_2)} m_{\gamma_1, \gamma_2}(q')$ .

The condition (2) is equivalent to  $m_{\gamma_1}(q) = m_{\gamma_2}(q)$  for any  $q \in \mathcal{C}(p_1, p_2)$ . Now let us discuss how to obtain such a  $\gamma_c = \{q(t) : t \in [0, T]\}$  as a parameterized flow

$$\dot{q}(t) = v(t), \quad t \in [0, T],$$

starting at an initial point  $q(0)$  that satisfies the condition (2) in Definition 3.2. The tangent vector  $v(t)$  will be carefully chosen, as follows.

Since the projections  $p_i(t) = p_{\gamma_i}(q(t))$  can be parameterized as

$$p_1(t) = p_{\gamma_1}(q(t)), \quad p_2(t) = p_{\gamma_2}(q(t))$$

the principal flows can also be parameterized as

$$\gamma_1 = \{p_1(t), t \in [0, T]\}, \quad \gamma_2 = \{p_2(t), t \in [0, T]\}.$$

Hence, we are equipped with two tangent vectors  $v_1(t) = \dot{p}_1(t)$  and  $v_2(t) = \dot{p}_2(t)$  at  $p_1(t)$  and  $p_2(t)$ , respectively. Numerically, the tangent vector  $v_1(t)$  or  $v_2(t)$  can be estimated by the vector field  $W(p_1(t))$  of  $\gamma_1$  at  $p_1(t)$  or the vector field  $W(p_2(t))$  of  $\gamma_2$  at  $p_2(t)$ .

The two tangent vectors  $v_1(t)$  and  $v_2(t)$  (or their estimates) may not necessarily lie on the same tangent plane at  $q(t)$  of  $\gamma_c$ . A natural solution is to move the tangent vectors towards the tangent plane at  $q(t)$  under a parallel transport along the geodesic curves. Let  $\tilde{v}_1(t)$  and  $\tilde{v}_2(t)$  be the transported tangent vectors of  $v_1(t)$  and  $v_2(t)$  respectively. In Appendix 2, we give the details of the machinery *Schild's Ladder* for an approximate implementation of the parallel transport.

As soon as the parallel transport is done at the current  $q(t)$ , the choice of  $v(t)$  is two-fold: 1) if  $v(t)$  lies in the plane spanned by  $\tilde{v}_1(t)$  and  $\tilde{v}_2(t)$ , then there is a  $\lambda(t)$  satisfying the equation  $v(t) = \lambda(t)\tilde{v}_1(t) + (1 - \lambda(t))\tilde{v}_2(t)$ ; 2) otherwise,  $v(t) \approx \lambda(t)\tilde{v}_1(t) + (1 - \lambda(t))\tilde{v}_2(t)$  with

$$\lambda(t) = \arg \min_{\lambda} \|v(t) - (\lambda\tilde{v}_1(t) + (1 - \lambda)\tilde{v}_2(t))\|_2,$$

where  $\|\cdot\|_2$  is the  $L_2$  norm.

Although the above discussion does not immediately yield an implementable estimation of the true vector  $v(t)$  ( $\lambda(t)$  is not available), it gives an updating rule of estimating  $v(t)$ , as follows. Prior to  $v(t)$ , we choose  $v(t - \delta)$  with a small  $\delta > 0$  and estimate  $\lambda(t)$  as

$$\lambda_{\delta}(t) = \arg \min_{\lambda} \|v(t - \delta) - (\lambda\tilde{v}_1(t) + (1 - \lambda)\tilde{v}_2(t))\|_2. \quad (8)$$

Then, we check if the estimate  $v_{\delta}(t) = \lambda_{\delta}(t)\tilde{v}_1(t) + (1 - \lambda_{\delta}(t))\tilde{v}_2(t)$  is acceptable or not via testing whether  $q_{\delta}(t)$ , the projection of  $q(t - \delta) + \delta v_{\delta}(t)$  onto the manifold, satisfies the conditions in Definition 3.2 under a given accuracy. If this is not the case, we slightly tune  $\lambda_{\delta}(t)$  to  $\lambda_{\delta}(t) := \lambda_{\delta}(t) \pm \epsilon$ , and check again until convergence. The updating can be that

$$\lambda_{\delta}(t) := \begin{cases} \lambda_{\delta}(t) + \epsilon & \text{if } m_{\gamma_1}(q_{\delta}(t)) < m_{\gamma_2}(q_{\delta}(t)); \\ \lambda_{\delta}(t) - \epsilon & \text{otherwise.} \end{cases} \quad (9)$$

Initially, when tangent vector  $v(0 - \delta)$  is not available for determining the initial  $\lambda_{\delta}(0)$ , we can simply choose  $\lambda_{\delta}(0) = 1/2$ . In the next section, we will present a detailed algorithm for computing the principal boundary.

## 4 Algorithm

Finding the principal boundary in practice can be more challenging than finding a principal flow, in the sense that the former problem is more attached to the picking of the points on the boundary. Recalling that for a point  $q \in \gamma_c$ ,

$$\min \{m_{\gamma_1}(q), m_{\gamma_2}(q)\} = \frac{1}{2} \{|m_{\gamma_1}(q) - m_{\gamma_2}(q)| + m_{\gamma_1}(q) + m_{\gamma_2}(q)\}$$

the minimum is achieved if and only if  $|m_{\gamma_1}(q) - m_{\gamma_2}(q)|$  is as small as possible. However, one cannot simply identify a sequence of such  $qs$  between the two flows to form an approximate boundary. The main reason is that we require the boundary to be a smooth curve. In this respect, we need a much more sophisticated mechanism to guarantee an equal margin on both sides of the boundary, including the choice of the initial point, whereas in the case of principal flow, picking the initial point can be very flexible. This is particularly true when the margins differ significantly between the two classes. In these cases, picking the mean or any symmetry of the data points is no longer meaningful. To facilitate the process of generating the boundary, we will require an initial point and then a process of fine-tuning the vector field along the way, which essentially has a direct impact on the principal boundary between the two flows.

We will now present a high-level description of the algorithm of computing the boundary (see Figure 1), the core of which is elaborated as follows.

Step 1 (*Initialising the boundary*): The initialisation involves finding a matching pair on  $\gamma_1$  and  $\gamma_2$ , and calculating an initial point  $q(0)$ . Arbitrarily choose a point  $c \in \gamma_2$ , and let  $p'_0 = p_{\gamma_1}(c)$  be the projection of  $c$  onto  $\gamma_1$ . Consider the geodesic curve  $g(c, p'_0)$  between  $c$  and  $p'_0$ . Obviously, for any point  $q \in g(c, p'_0)$ , we always have  $p'_0 = p_{\gamma_1}(q)$ . Let  $p''_0 = p_{\gamma_2}(q)$  be the projection of  $q$  onto  $\gamma_2$ . Hence, identify  $q_0 \in g(c, p'_0)$  such that,

$$d_{\mathcal{M}}(q_0, \gamma_1) - \sigma_{\gamma_1}(p'_0) = d_{\mathcal{M}}(q_0, \gamma_2) - \sigma_{\gamma_2}(p''_0).$$

Here, we call  $q_0$  a warm start. Pick a matching pair as follows

$$p_1(0) = p'_0, \quad p_2(0) = p''_0$$

Then we can identify a point  $q(0) \in g(p'_0, p''_0)$  such that  $m_{\gamma_1}(q(0)) = m_{\gamma_2}(q(0))$ . Obviously,  $q(0)$  satisfies the conditions in Definition 3.2.

Step 2 (*Updating the boundary*): Calculating  $q(t)$  for a  $t > 0$  from the previous point  $q(t - \delta)$  with a small  $\delta > 0$ . Initially, let  $\tilde{v}_1(t) = \dot{p}_1(t)$ ,  $\tilde{v}_2(t) = \dot{p}_2(t)$ , and set  $\lambda_\delta(t)$  as in (8). Then, estimate  $v(t)$  by

$$v_\delta(t) = \lambda_\delta(t)\tilde{v}_1(t) + (1 - \lambda_\delta(t))\tilde{v}_2(t), \quad (10)$$

and find the projection as

$$q_\delta(t) = \exp_{q(t-\delta)}(q(t-\delta) + \delta v_\delta(t)). \quad (11)$$

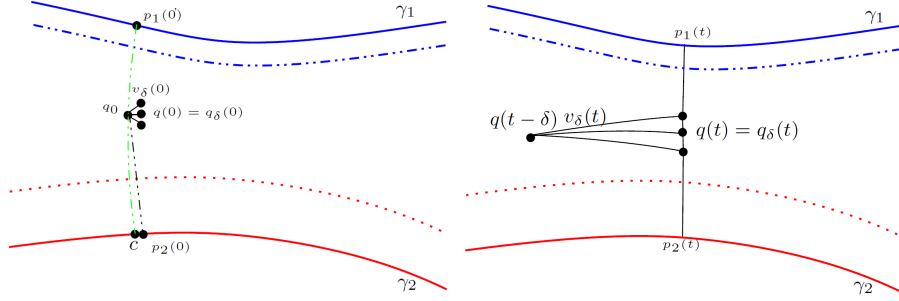


Figure 1: Algorithm. (a) Step 1 (Initializing the boundary):  $q_0$  is the warm start for finding the matching pair  $p_1(0)$  and  $p_2(0)$ ;  $q(0)$  is the initial point chosen from the projection  $q_\delta(0) = \mathbf{exp}_{q_0}(q_0 + \delta v_\delta(0))$  satisfying the conditions of Definition 3.2, via alternating  $v_\delta(0)$ . (b) Step 2 (Updating the boundary):  $q(t-\delta)$  is used to find  $q(t)$ ;  $q(t)$  is chosen by from the projection  $q_\delta(t) = \mathbf{exp}_{q(t-\delta)}(q(t-\delta) + \delta v_\delta(t))$  satisfying the conditions of Definition 3.2, via alternating  $v_\delta(t)$ .

If  $q_\delta(0)$  satisfies the conditions in Definition 3.2, let  $q(t) = q_\delta(t)$ ; otherwise, update  $\lambda_\delta(t)$  by (9), and re-calculate  $v_\delta(t)$  in (10) and  $q_\delta(t)$  in (11).

The algorithm will be executed for a period of time and it produces a sequence of  $\{q(t)\}$ . The constructed sequence is indeed the principal boundary since we always have that for every  $q(t) \in \gamma_c$ ,  $p_1(t) = p_{\gamma_1}(q(t))$ , and  $p_2(t) = p_{\gamma_2}(q(t))$ ,

$$d_{\mathcal{M}}(q(t), \gamma_1) - \sigma_{\gamma_1}(p_1(t)) = d_{\mathcal{M}}(q(t), \gamma_2) - \sigma_{\gamma_2}(p_2(t)).$$

Supposing we may discretise the  $\gamma_c$  as  $\gamma_c = (q(0), \dots, q(N))$ ,  $q(i) \in \mathcal{M}$ . The length of the principal boundary can be numerically approximated

$$\ell(\gamma_c) \approx \sum_{i=0}^{N-1} d_{\mathcal{M}}(q(i), q(i+1)).$$

## 5 Property of the principal boundary

This section shows that the local segment of the principal boundary reduces to the boundary given by the support vector machine. We remark here that the SVM boundary we use here is a manifold extension of the usual SVM, which is essentially a geodesic curve. The same results hold in the context of Euclidean spaces, where  $\mathcal{M}$  is a linear subspace of  $\mathbb{R}^d$ . By making the notion of “local equivalence” precise, we provide a measure of distance between the principal boundary, obeying Definition 3.2 and the SVM boundary.

To study the relation, we start with a quantitative description of the segment of  $\gamma_c$  on  $\mathcal{M}$  by the following proposition.

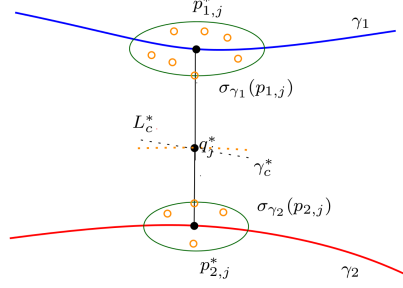


Figure 2: The principal boundary  $\gamma_c^*$  in the local configuration. The covering ellipse ball (in green) with the second radius  $\sigma_{\gamma_1}(p_{1,j})$ , centered at  $p_{1,j}^*$  contain the local points (in “o”) for class +1; the shortest distance between  $q_j^*$  and the corresponding local configuration of class +1 is approximated by  $d_{\mathcal{M}}(p_{1,j}^*, q_j^*) - \sigma_{\gamma_1}(p_{1,j})$  (same for class -1).

**Proposition 5.1** (*Local configuration*) Consider a small segment  $\gamma_c^*$  of  $\gamma_c$  on  $\mathcal{M}$ . Suppose that

1. The segment is discretised as  $\gamma_c^* = \{q_1^*, \dots, q_M^*\}$ , where  $q_j^* \in \mathcal{M}$ .
2. Following the notation in Section 3.1, let  $\mathcal{N}(p_{1,j}^*, h)$  be the set of samples in the  $h$ -neighbourhood of  $p_{1,j}^*$ . Clearly, the  $M$  local neighbourhoods give a configuration of local data points from class +1 as

$$\cup_{j=1}^M \mathcal{N}(p_{1,j}^*, h) = \{x_{1,1}, \dots, x_{1,k_1}\}.$$

Similarly, we can define  $\{x_{2,1}, \dots, x_{2,k_2}\}$  for the other class -1.

If  $\gamma_c^*$  is small enough, it is approximately a segment of a straight line  $L_c^*$ , and  $q_j^*$ 's are located at the line, also approximately. Let the projections of  $q_j^*$  onto  $\gamma_1$  and  $\gamma_2$  be

$$\gamma_1^* = \{p_{1,1}^*, \dots, p_{1,M}^*\}, \quad \gamma_2^* = \{p_{2,1}^*, \dots, p_{2,M}^*\}$$

respectively. The SVM on the two classes determines a geodesic curve  $L_{\text{svm}}$  that separates the two sets, such that the margin of  $L_{\text{svm}}$

$$m(L_{\text{svm}}) = \min \left\{ \min_k d_{\mathcal{M}}(x_{1,k}, L_{\text{svm}}), \min_k d_{\mathcal{M}}(x_{2,k}, L_{\text{svm}}) \right\}$$

is maximised. For  $\gamma_c^*$ , we define the margin as

$$m(\gamma_c^*) = \min \left\{ \min_k d_{\mathcal{M}}(x_{1,k}, \gamma_c^*), \min_k d_{\mathcal{M}}(x_{2,k}, \gamma_c^*) \right\}.$$

To quantify the relation of  $m(\gamma_c^*)$  and  $m(L_{\text{svm}})$ , we will basically need three approximations. We remark here that although a careful approximation of  $\gamma_c^*$  to  $L_{\text{svm}}$  can be bounded under some error assumptions, together with an estimation

of  $m(\gamma_c^*) \approx m(L_c^*)$ , doing so would result in a complicated analysis. To simplify our discussion, we will first sketch an overall review of the local equivalence while highlighting the idea. A refined approximation is followed in terms of Theorem 1.

Let us consider samples in each neighbour set  $\mathcal{N}(p_{1,j}^*, h)$ . Assume that these neighbours are covered by an ellipse ball of the second radius being  $\sigma_{\gamma_1}(p_{1,j})$ , centred at  $p_{1,j}^*$ . Since  $d_{\mathcal{M}}(p_{1,j}^*, q_j^*) - \sigma_{\gamma_1}(p_{1,j}) = m_{\gamma_1}(q_j^*)$ , the quantity

$$\min_{x_{1,k} \in \mathcal{N}(p_{1,j}^*, h)} d_{\mathcal{M}}(x_{1,k}, \gamma_c^*) \approx m_{\gamma_1}(q_j^*). \quad (12)$$

should approximately hold, up to some degree. From  $\min_k d_{\mathcal{M}}(x_{1,k}, \gamma_c^*) = \min_j \min_{x_{1,k} \in \mathcal{N}(p_{1,j}^*, h)} d_{\mathcal{M}}(x_{1,k}, \gamma_c^*)$ , we get that

$$\min_k d_{\mathcal{M}}(x_{1,k}, \gamma_c^*) \approx \min_j m_{\gamma_1}(q_j^*).$$

Similarly, we also have that  $\min_k d_{\mathcal{M}}(x_{2,k}, \gamma_c^*) \approx \min_j m_{\gamma_2}(q_j^*)$ . Therefore, we have

$$m(\gamma_c^*) \approx \min_j \{m_{\gamma_1}(q_j^*), m_{\gamma_2}(q_j^*)\} = \min_j m_{\gamma_1, \gamma_2}(q_j^*).$$

On the other hand, let  $q'_j$  be the intersected point of the geodesic curve  $\mathcal{C}(p_{1,j}^*, p_{2,j}^*)$  and the straight line  $L_{\text{svm}}$ . We also have the approximations that

$$\min_{x_{1,k} \in \mathcal{N}(p_{1,j}^*, h)} d_{\mathcal{M}}(x_{1,k}, L_{\text{svm}}) \approx d_{\mathcal{M}}(p_{1,j}^*, q'_j) - \sigma_{\gamma_1}(p_{1,j}) = m_{\gamma_1}(q'_j), \quad (13)$$

$$\min_{x_{2,k} \in \mathcal{N}(p_{2,j}^*, h)} d_{\mathcal{M}}(x_{2,k}, L_{\text{svm}}) \approx d_{\mathcal{M}}(p_{2,j}^*, q'_j) - \sigma_{\gamma_2}(p_{2,j}) = m_{\gamma_2}(q'_j). \quad (14)$$

It follows that the SVM margin

$$\begin{aligned} m(L_{\text{svm}}) &= \min_j \min \left\{ \min_{x_{1,k} \in \mathcal{N}(p_{1,j}^*, h)} d_{\mathcal{M}}(x_{1,k}, L_{\text{svm}}), \right. \\ &\quad \left. \min_{x_{2,k} \in \mathcal{N}(p_{2,j}^*, h)} d_{\mathcal{M}}(x_{2,k}, L_{\text{svm}}) \right\} \\ &\approx \min_j \min \{m_{\gamma_1}(q'_j), m_{\gamma_2}(q'_j)\} = \min_j m_{\gamma_1, \gamma_2}(q'_j) \\ &\leq \min_j \max_{q \in \mathcal{C}(p_{1,j}^*, p_{2,j}^*)} m_{\gamma_1, \gamma_2}(q) = \min_j m_{\gamma_1, \gamma_2}(q_j^*) = m(\gamma_c^*). \end{aligned}$$

Let  $L_c^*$  be a geodesic curve nearest by  $\gamma_c^*$ . Then  $m(\gamma_c^*) \approx m(L_c^*)$ , and

$$m(L_{\text{svm}}) \lesssim m(\gamma_c^*) \approx m(L_c^*) \leq m(L_{\text{svm}})$$

by definition, which suggests that  $L_{\text{svm}}$  approximately coincides with  $\gamma_c^*$ .

Obviously, it can be seen that the local equivalence holds if Approximation (12) and (13) (or (14)) are satisfactory. We introduce the following condition to guarantee the approximations up to some quantitative degree of uncertainty. This is done by linking the density of sample points in a local neighbour with a probability measure.

**Condition 5.1** (*Covering ellipse ball*) For each  $p_{1,j}^*$ , consider samples in each neighbour set  $\mathcal{N}(p_{1,j}^*, h)$ . We assume that,

1.  $\mathcal{N}(p_{1,j}^*, h)$  has  $k_{1,j}$  neighbours that are covered by an ellipse ball of the second radius  $\sigma_{\gamma_1}(p_{1,j})$ , centred at  $p_{1,j}^*$ ,
2. when  $k_{1,j} \rightarrow \infty$ , with probability of at least  $1 - o(\frac{1}{\sqrt{k_{1,j}}})$

$$\left| \min_{x_{1,k} \in \mathcal{N}(p_{1,j}^*, h)} d_{\mathcal{M}}(x_{1,k}, \gamma_c^*) - m_{\gamma_1}(q_j^*) \right| \leq \sqrt{\frac{\log k_{1,j}}{k_{1,j}}};$$

$$\left| \min_{x_{1,k} \in \mathcal{N}(p_{1,j}^*, h)} d_{\mathcal{M}}(x_{1,k}, L_{\text{svm}}) - m_{\gamma_1}(q'_j) \right| \leq \sqrt{\frac{\log k_{1,j}}{k_{1,j}}},$$

3. similar conditions apply to class  $-1$ .

**THEOREM 1** Let  $\gamma_c^*$  and  $L_{\text{svm}}$  be the separating boundary between the local samples of two classes, derived by the principal boundary and SVM, respectively. Let  $k = \min_{i,j} k_{i,j}$  where  $i = 1, 2$  and  $j = 1, \dots, M$ . Given Proposition 5.1 and Condition 5.1,  $\gamma_c^*$  and  $L_{\text{svm}}$  are equivalent such that  $m(\gamma_c^*) = m(L_{\text{svm}})$ , with probability of at least  $1 - o(\frac{1}{\sqrt{k}})$ , for  $k \rightarrow \infty$ .

Theorem 1 gives an equivalence of  $\gamma_c^*$  and  $L_{\text{svm}}$  on the curved manifold. The proof of Theorem 1 is given in Appendix 1. Although we have potentially linked  $L_{\text{svm}}$  with  $\gamma_c^*$  with an interest of interpreting them locally, it does not necessarily mean that Theorem 1 is only valid when the locality is infinitesimal. Instead, it is governed by the spacings of the segment  $\gamma_c^*$ . In fact, when the locality of  $\gamma_c^*$  is not infinitesimal, the equivalence still holds between  $L_c^*$  and  $L_{\text{svm}}$ , provided that  $L_c^*$  is close to  $\gamma_c^*$ . In case of a flat manifold, the results still hold, where both  $L_{\text{svm}}$  and  $\gamma_c^*$  are reduced to straight lines, and  $\gamma_c^*$  is a curve close to them.

## 6 Simulation

To illustrate the principal boundary as being dependent on the configuration of the data sets, we first generate two sets of noisy data on  $S^2 \subset \mathbb{R}^3$ . We claim here that choosing the sphere as a test manifold is done only for simplicity, as it stands for the most common manifold that one can work with and compare with other methods. By tuning the vector field along the principal flow of the two data sets, we visualise the evolution of the principal boundary. We remark here that the principal flows are the modified principal flows in (7) for the labelled data. Figure 3 shows the labelled data (Figure 3(a)), the super-imposed principal flows (Figure 3(b)), and the principal boundary (Figure 3(c-d)). In the step of initialising the boundary, the initial point (in red) has been obtained from the warm start (in blue); both of them are labelled in Figure 3(c). In Figure 3(b), the two green curves are the estimated deviation of the principal flows, providing a measure of the margin of the flow. The boundary enables itself to bend wherever the vector field of the two flows changes. This can be seen from the vectors (in red/black arrows) of Figure 3(d), where they are optimised towards a direction of achieving the maximum margin between the two flows, a criterion introduced in the step of updating the boundary.

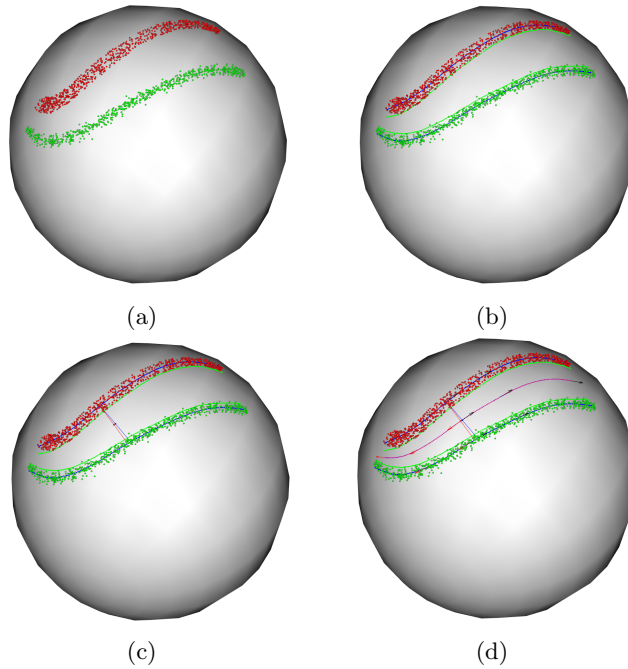


Figure 3: Plots of the principal boundary: (a) plot of data. (b) modified principal flow fitted to the data with an estimated margin. (c) initialisation of the boundary. (d) full path of the principal boundary.



We also contrast the principal boundary with the boundary by the SVM classifier on the same set of data. We generate the SVM boundary by performing an SVM classifier, separating the data in the Euclidean space and then mapping it back onto the manifold. By avoiding explicit mapping in SVM, four kernels (Gaussian radial basis function (Gaussian RBF), linear, polynomial and sigmoid) have been used with the SVM in training the classification machine. Their performances have been compared with the principal boundary and the result is reported in Figure 4. Among all of the experiments, the principal boundary (in purple) goes through the initial point (in red), remaining a equal margin between the two labelled data sets. The SVM finds the boundary quite differently in all four cases: the best boundary by SVM is the one with RBF (in light blue), in that it is the closest one to the principal boundary, except the left part (Figure 4(a)); the linear kernel (in pink) in does a decent job in the middle part of the data but clearly could not handle the curvature on the two ends (Figure 4(b)); both the polynomial (in grey) and sigmoid (in orange) kernels fail to achieve a reasonable boundary (Figure 4 (c), (d)) on the manifold. More experiments of the SVM boundary with varying parameters under different kernels can be found in the Appendix 7. This example shows the impact of the resulting SVM boundary by choosing different kernel functions in SVM. If the choice of kernel is done in advance, it can be seen that SVM performs relatively well (i.e., in this case, when the Gaussian RBF kernel is chosen) compared to the principal boundary. However, very often, one is not given an indication of which kernel to use when performing the classification by SVM. In this sense, it is suggested that the principal boundary method could be a wise choice when the data clearly has a structure.

Though the SVM boundary above seems to be a reasonable means of understanding the principal boundary, a refined SVM boundary has also been investigated. In line with the setting of local configuration 5.1, we have obtained a piecewise SVM boundary for this same set of data. This boundary is constructed by performing the SVM process on each pair of the corresponding neighbourhoods from the two classes. In this sense, the refined boundary is a local version of the previous SVM boundary. As showed in the proof of Theorem 1, the local SVM is performed on each paired neighbourhood—essentially, it is a geodesic segment or rough line segment, there is no significant difference in choosing the type of kernel. Figure 5 shows the piecewise SVM boundary at each locality parameter  $h \in (.05, .1, .15, .2)$  via linear kernel. It is expected that the piecewise SVM boundary would not necessarily produce a smooth boundary, as we observe that when  $h$  increases, the discontinuity of the boundary improves, with a common trend that all SVM segments as a whole are aligned closer to the principal boundary. Although this does not necessarily suggest the existence of an optimal  $h$  here, we do see that this behaviour matches well with that of the aforementioned Theorem 1.

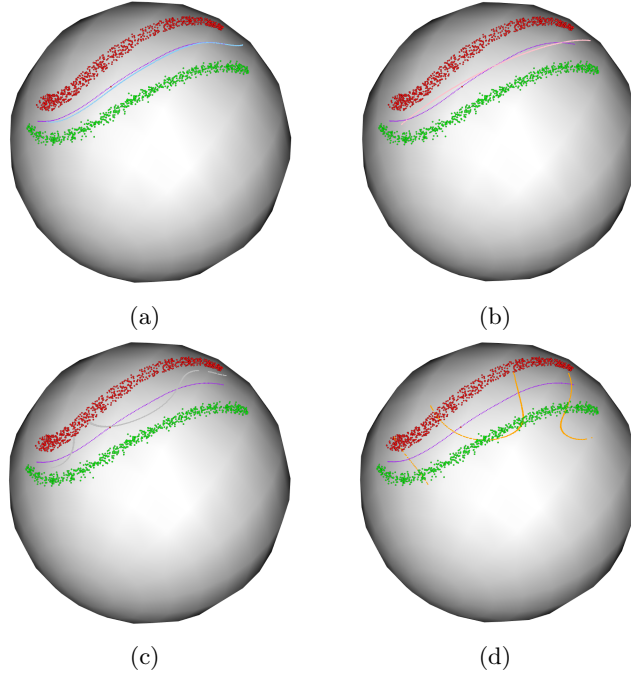


Figure 4: SVM boundary and principal boundary on the unit sphere: (a) SVM boundary (Gaussian RBF) and principal boundary. (b) SVM boundary (linear) and principal boundary. (c) SVM boundary (polynomial) and principal boundary. (d) SVM boundary (sigmoid) and principal boundary. All kernel functions except linear have been used with default parameters: bandwidth  $\gamma = 1/4$  and Lagrange multiplier  $C = 1$ . For polynomial, the degree parameter  $df = 3$ . For polynomial and sigmoid, the coefficient parameter  $c_0 = 0$ .

## 7 Conclusion

The classification problem for data points on non-linear manifolds is a very challenging topic and it plays an increasingly important role in real-world problems. Conventional approaches, such as SVM in the Euclidean space, are essentially unhelpful for either learning the structure of the underlying manifold or deciding the boundary directly on the manifold. The main reason for this lies in the fact that those approaches simply do not use the local geometric information of the manifold.

With the aim of finding a new method for classifying data points with labels on manifolds, we have described a general framework. The key techniques we have used are the tangent space at a given point of the principal flow, which in principle represents the local geometry of the data variation. In words, the type of local geometric structure we use is local vector fields of the principal flow. We showed the necessity of estimating the margin between the boundary and

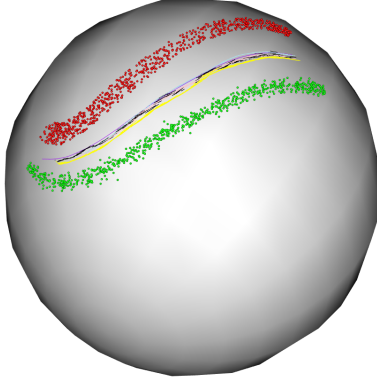


Figure 5: Performance of piecewise SVM boundary and the principal boundary. The piecewise SVM boundary with different  $h$  are plotted in black ( $h = .05$ ), yellow ( $h = .1$ ), pink ( $h = .15$ ) and light-blue ( $h = .2$ ). The principal boundary (purple) is also superimposed.

the flows from a classification perceptive. The combination of fine-tuning the vector fields and the margin provides the alignment of the local data geometry and the global coordinates of the boundary on the manifold. The principal boundary was seen to be interpretable as a local equivalence of the classification boundary by SVM. We provided an error analysis to exhibit the equivalence between them, by linking the data density and noise level with a probability measure. Examples are sketched related to the implemented algorithm of the principal boundary and the numerical comparison with that process by SVM (global SVM and piecewise SVM). We claim here, that although by Theorem 1 the principal boundary coincides with the SVM locally, in practice, they appear to be quite different as the basis (kernel) functions one would use in SVM are usually unknown.

The formulation of the principal boundary can be extended to several lines of research. From the theoretical point of view, Condition 5.1 (covering ellipse ball) essentially can be relaxed to suit the needs of the analysis for a finite sample. This, if it can be done with a detailed error analysis, would potentially help us understand the boundary better and improve accuracy. From the application point of view, this new method has the potential to be a useful tool for real data analysis. Certainly, a successful classification also depends on 1) the data configuration; 2) the noise. If the labelled data on the manifold are overlapping, one might consider using penalty functions. Some of the results in non-parametric regression or machine learning will be helpful in this respect, and as this is one of our ongoing works, we will investigate it in the future.

## Appendix 1: Proof of Theorem 1

**Proof** Let  $\phi_{i,j} = \min_{x_{i,k} \in \mathcal{N}(p_{i,j}^*, h)} d_{\mathcal{M}}(x_{i,k}, \gamma_c^*) - m_{\gamma_i}(q_j^*)$  for  $i = 1, 2$ . Then

$$\min_k d_{\mathcal{M}}(x_{i,k}, \gamma_c^*) = \min_j \min_{x_{i,k} \in \mathcal{N}(p_{i,j}^*, h)} d_{\mathcal{M}}(x_{i,k}, \gamma_c^*) = \min_j \{m_{\gamma_i}(q_j^*) + \phi_{i,j}\}.$$

Under Condition 5.1, with probability of at least  $1 - o(\frac{1}{\sqrt{k_{i,j}}})$ ,  $|\phi_{i,j}| \leq \sqrt{\frac{\log k_{i,j}}{k_{i,j}}}$ .

Hence, with probability of at least  $\min_j (1 - o(\frac{1}{\sqrt{k_{i,j}}})) = 1 - o(\frac{1}{\sqrt{\min_j k_{i,j}}})$

$$|\min_k d_{\mathcal{M}}(x_{i,k}, \gamma_c^*) - \min_j m_{\gamma_i}(q_j^*)| \leq \max_j |\phi_{i,j}| = \phi^*.$$

Therefore, if we define the margin as

$$m(\gamma_c^*) = \min \left\{ \min_k d_{\mathcal{M}}(x_{1,k}, \gamma_c^*), \min_k d_{\mathcal{M}}(x_{2,k}, \gamma_c^*) \right\},$$

then with probability of at least  $1 - o(\frac{1}{\sqrt{k}})$  with  $k = \min_{i,j} k_{i,j}$ , we have

$$|m(\gamma_c^*) - \min_j m_{\gamma_1, \gamma_2}(q_j^*)| \leq \phi^*.$$

since  $m_{\gamma_1, \gamma_2}(q_j^*) = m_{\gamma_i}(q_j^*)$  for  $i = 1, 2$ .

On the other hand, assume that the geodesic curve  $\mathcal{C}(p_{1,j}^*, p_{2,j}^*)$  intersects  $L_{\text{svm}}$  at  $q'_j$ . Then, we also have that

$$\begin{aligned} \min_{x_{1,k} \in \mathcal{N}(p_{1,j}^*, h)} d_{\mathcal{M}}(x_{1,k}, L_{\text{svm}}) &= d_{\mathcal{M}}(p_{1,j}^*, q'_j) - \sigma_{\gamma_1}(p_{1,j}^*) = m_{\gamma_1}(q'_j), \\ \min_{x_{2,k} \in \mathcal{N}(p_{2,j}^*, h)} d_{\mathcal{M}}(x_{2,k}, L_{\text{svm}}) &= d_{\mathcal{M}}(p_{2,j}^*, q'_j) - \sigma_{\gamma_2}(p_{2,j}^*) = m_{\gamma_2}(q'_j). \end{aligned}$$

It follows that

$$\begin{aligned} m(L_{\text{svm}}) &= \min_j \min \left\{ \min_{x_{1,k} \in \mathcal{N}(p_{1,j}^*, h)} d_{\mathcal{M}}(x_{1,k}, L_{\text{svm}}), \right. \\ &\quad \left. \min_{x_{2,k} \in \mathcal{N}(p_{2,j}^*, h)} d_{\mathcal{M}}(x_{2,k}, L_{\text{svm}}) \right\} \\ &= \min_j \min \{m_{\gamma_1}(q'_j), m_{\gamma_2}(q'_j)\} = \min_j m_{\gamma_1, \gamma_2}(q'_j) \\ &\leq \min_j \max_{q \in \mathcal{C}(p_{1,j}^*, p_{2,j}^*)} m_{\gamma_1, \gamma_2}(q) = \min_j m_{\gamma_1, \gamma_2}(q_j^*) = m(\gamma_c^*). \end{aligned}$$

Let  $L_c^*$  be a geodesic curve nearest by  $\gamma_c^*$ . Then  $m(\gamma_c^*) \approx m(L_c^*)$ , and

$$m(L_{\text{svm}}) \leq m(\gamma_c^*) \approx m(L_c^*) \leq m(L_{\text{svm}})$$

where the last inequality holds by definition, which together suggests that  $L_{\text{svm}}$  approximately coincides with  $\gamma_c^*$ .

## Appendix 2: Parallel transport of the tangent vector

Denote a curve  $\gamma \in \mathcal{M}$ . Consider the two points  $p, q \in \gamma$ . Let  $v$  be a unit vector at  $p$ . The following algorithm parallel transports  $v$  at  $p$  to  $q$ :

- (0) Define the geodesic starting from  $p$  with  $v$  and ending at  $p_1$ , so that the geodesic segment  $\mathcal{C}(p, p_1)$  has a unit length,
- (1) Choose a point  $p_2 \in \gamma$  that is close to  $p$ , and connect  $p_1$  and  $p_2$  by a geodesic segment  $\mathcal{C}(p_1, p_2)$ ,
- (2) Pick the middle point  $p_3$  on  $\mathcal{C}(p_1, p_2)$  in the sense that the segments  $\mathcal{C}(p_1, p_3)$  and  $\mathcal{C}(p_2, p_3)$  take equal lengths (i.e.,  $d_{\mathcal{M}}(p_1, p_3) = d_{\mathcal{M}}(p_2, p_3)$ ),
- (3) Connect  $p$  and  $p_3$  by a geodesic  $\mathcal{C}(p, p_3)$ , extend the same geodesic until its curve length doubles, reaching  $p_4$ , then connect  $p_2$  and  $p_4$  by a geodesic  $\mathcal{C}(p_2, p_4)$ ,
- (4) If  $d_{\mathcal{M}}(p_2, q) < \epsilon$ , terminate the procedure (the tangent  $v'$  at  $p_2$  to this geodesic,  $\mathcal{C}(p_2, p_4)$ , is the parallel transport of  $v$  to  $p_2$ ); otherwise iterate Steps (0)-(3) in a sufficient number of small steps.

## Appendix 3: Experiments of SVM boundary with different kernels

## References

- [1] D. L. Donoho and C. Grimes. Hessian eigenmaps: New locally linear embedding techniques for high-dimensional data. *Proceedings of the National Academy of Sciences (PNAS)*, 102:7426–7431, 2003.
- [2] P. T. Fletcher and S. Joshi. Riemannian geometry for the statistical analysis of diffusion tensor data. *Signal Processing*, 87:250–262, 2007.
- [3] P. T. Fletcher, C. Lu, S. M. Pizer, and S. Joshi. Principal geodesic analysis for the study of nonlinear statistics of shape. *IEEE Transactions on Medical Imaging*, 23:995–1005, 2004.
- [4] M. Fréchet. Les éléments aléatoires de nature quelconque dans un espace distancié. *Annales de l’Institut Henri Poincaré*, 10:215–310, 1948.
- [5] S. Gerber, T. Tasdizen, P. T. Fletcher, S. Joshi, R. Whitaker, and the Alzheimers Disease Neuroimaging Initiative (ADNI). Manifold modeling for brain population analysis. *Medical Image Analysis*, 14:643–653, 2010.
- [6] S. Huckemann, T. Hotz, and A. Munk. Intrinsic shape analysis: Geodesic pca for riemannian manifolds modulo isometric lie group actions. *Statistica Sinica*, 20:1–100, 2010.
- [7] S. Huckemann and H. Ziezold. Principal component analysis for riemannian manifolds, with an application to triangular shape spaces. *Advances in Applied Probability*, 38:299–319, 2006.
- [8] S. Jung, I. L. Dryden, and J. S. Marron. Analysis of principal nested spheres. *Biometrika*, 99:551–568, 2012.
- [9] P. E. Jupp and J. T. Kent. Fitting smooth paths to spherical data. *Journal of the Royal Statistical Society, Series C*, 36:34–36, 1987.
- [10] D. G. Kendall, D. Barden, T. K. Carne, and H. Le. *Shape and Shape Theory*. Wiley, New York, 1999.
- [11] K. Kenobi, I. L. Dryden, and H. Le. “shape curves and geodesic modelling. *Biometrika*, 97:567–584, 2010.
- [12] A. Kume, I. L. Dryden, and H. Le. Shape-space smoothing splines for planar landmark data. *Biometrika*, 94:513–528, 2007.
- [13] H. Liu, Z. Yao, S. Leung, and T. F. Chan. A level set based variational principal flow method for nonparametric dimension reduction on riemannian manifolds. *SIAM Journal on Scientific Computing*, 39:369–376, A1616–A1646.
- [14] V. M. Panaretos, T. Pham, and Z. Yao. Principal flows. *Journal of the American Statistical Association*, 109:424–436, 2014.

- [15] X. Pennec. Intrinsic statistics on riemannian manifolds: Basic tools for geometric measurements. *Journal of Mathematical Imaging and Vision*, 25:127–154, 2006.
- [16] X. Pennec and J.-P. Thirion. A framework for uncertainty and validation of 3d registration a framework for uncertainty and validation of 3d registration methods based on points and frames. *Int. Journal of Computer Vision*, 25:203–229, 1997.
- [17] S. T. Roweis and L. K. Sau. Nonlinear dimensionality reduction by locally linear embedding. *Science*, 290:369–376, 23232326.
- [18] R. Souvenir and R. Pless. Image distance functions for manifold learning. *Image and Vision Computing*, 25(3):365–373, 2007.
- [19] Z. Yao and T. Pham. Principal sub-manifolds. *Manuscript*, 2016.
- [20] Z. Zhang and H. Zha. Principal manifolds and nonlinear dimensionality reduction via tangent space alignment. *SIAM journal on scientific computing*, 26(1):313–338, 2004.

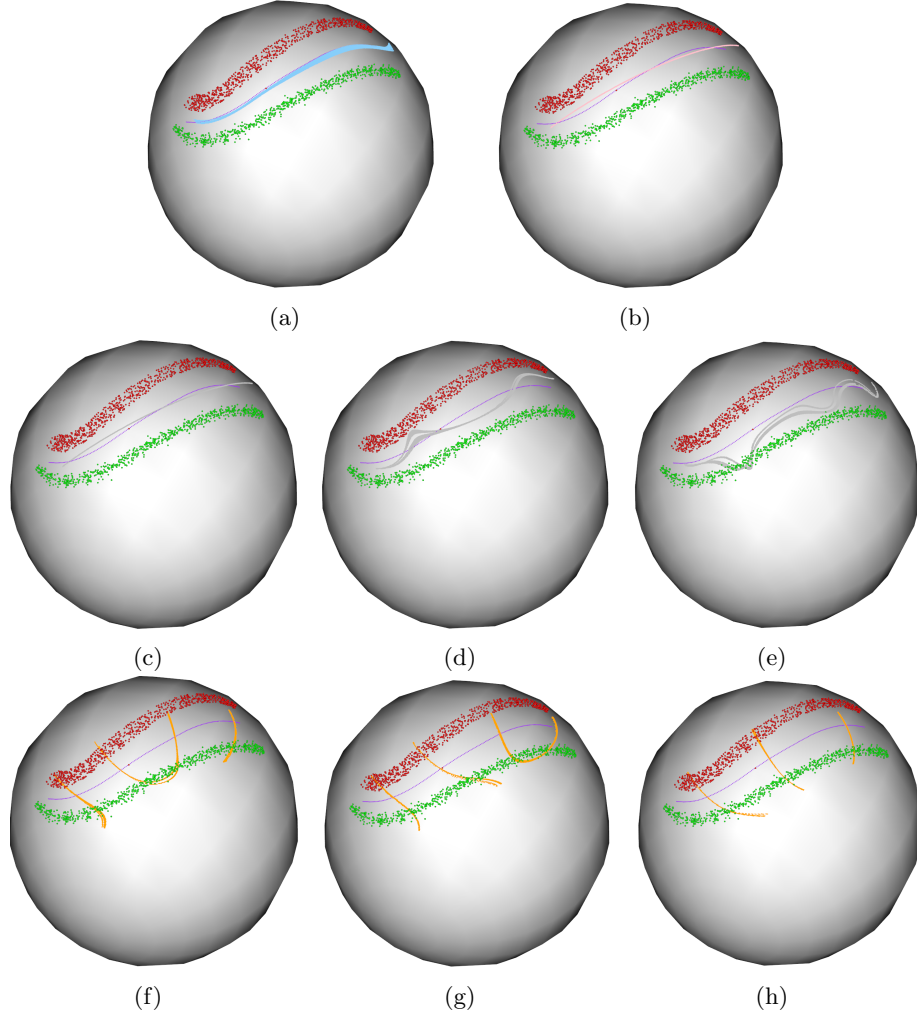


Figure 6: SVM boundary with different kernels on unit sphere: (a) plots of SVM boundary (Gaussian RBF) for varying bandwidth  $\gamma \in (.1, 1)$  and Lagrange multiplier  $C \in (.1, 1)$ . (b) SVM boundary (linear) for Lagrange multiplier  $C \in (.1, 1)$ . (c)-(e) SVM boundary (polynomial) for varying bandwidth  $\gamma \in (.1, 1)$  and Lagrange multiplier  $C \in (.1, 1)$  with degree parameter  $df = 1$ (c),  $df = 3$ (d) and  $df = 5$ (e), respectively. (f)-(h) SVM boundary (sigmoid) for varying bandwidth  $\gamma \in (.1, 1)$  and Lagrange multiplier  $C \in (.1, 1)$  with coefficient parameter  $c_0 = 0$  (f),  $c_0 = .5$ (g) and  $c_0 = 1$ (h), respectively. All plots are superimposed with the principal boundary.